Current Opinion in Solid State and Materials Science 18 (2014) 253–261

Contents lists available at ScienceDirect

Current Opinion in Solid State and Materials Science

journal homepage: www.elsevier.com/locate/cossms

Grain boundary segregation engineering in metallic alloys: A pathway to the design of interfaces

D. Raabe *, M. Herbig, S. Sandlöbes, Y. Li, D. Tytko, M. Kuzmina, D. Ponge, P.-P. Choi

Max-Planck-Institut für Eisenforschung, Department for Microstructure Physics and Alloy Design, Max-Planck-Str. 1, 40237 Düsseldorf, Germany

ARTICLE INFO

Article history:
Received 24 March 2014
Revised 3 June 2014
Accepted 8 June 2014
Available online 27 June 2014

Keywords:
Grain boundary
Atom probe tomography
Segregation
Phase transformation

ABSTRACT

Grain boundaries influence mechanical, functional, and kinetic properties of metallic alloys. They can be manipulated via solute decoration enabling changes in energy, mobility, structure, and cohesion or even promoting local phase transformation. In the approach which we refer here to as 'segregation engineering' solute decoration is not regarded as an undesired phenomenon but is instead utilized to manipulate specific grain boundary structures, compositions and properties that enable useful material behavior. The underlying thermodynamics follow the adsorption isotherm. Hence, matrix-solute combinations suited for designing interfaces in metallic alloys can be identified by considering four main aspects, namely, the segregation coefficient of the decorating element; its effects on interface cohesion, energy, structure and mobility; its diffusion coefficient; and the free energies of competing bulk phases, precipitate phases or complexions. From a practical perspective, segregation engineering in alloys can be usually realized by a modest diffusion heat treatment, hence, making it available in large scale manufacturing.

Introduction and motivation

Grain boundaries (GBs) are ubiquitous defects in metallic alloys governing a range of properties, such as tensile strength, fatigue resistance, fracture toughness, strain hardening, brittleness, conductivity, or corrosion [1–7].

Unlike bulk phases they are planar and require 5 parameters to be crystallographically characterized (disorientation, plane inclination). Hence, they cannot be regarded as scalar objects with homogeneous properties but as a high dimensional class of defects. For example, even for highly coherent GBs such as first order twins (Σ3 CSL (coincidence site lattice)) exponential property changes can occur if the GB plane is misaligned by only a few degrees from its most coherent position.

GBs can either weaken (inter-crystalline fracture, stress corrosion cracking) or strengthen (Hall-Petch effect) polycrystalline metallic materials. In either case the types of GBs involved affect the specific material response substantially as was discussed particularly in the context of highly coherent versus random GBs. These observations led to the concept of grain boundary engineering which aims at designing polycrystals with specific GB distributions [8–11].

The next logical step in this context lies in also considering and engineering the segregation and its effects on GBs [12–24]. This is an obvious thought since many if not all GB properties are accessible to decoration-driven manipulation such as cohesion [12–14]; energy [18–23]; fracture resistance [12]; electrical conductivity [25,26]; transport coefficients [27]; electrochemical properties [24,25,28]; hydrogen embrittlement [30,31]; mobility [32–38]; and resistance to or sources of dislocations [47–57] to name only a few effects that are relevant for structural alloys.

We refer to such manipulation of GBs via solute decoration and even confined transformation as 'grain boundary segregation engineering' (GBSE) or just 'segregation engineering' [58]. Applying GBSE needs to involve both, thermodynamic (segregation coefficient; co-segregation; competing bulk phases) and kinetic (diffusion) influence factors. Hence, not only the associated crystallographic degrees of freedom and all segregated elements should be considered but also time and temperature. However, as will be addressed below, GBSE can for a number of alloys even be applied when knowing the average segregation level to non-ordered or 'random' GBs, i.e., a full 5D crystallographic description is not in all cases required. GB segregation changes with time when the heat treatment or application temperature is high enough for diffusion. Hence, also the GB properties may alter. GBSE considers solute decoration not as an undesired and inherited phenomenon but instead utilizes segregation as a tool for site-specific manipulation that allows for optimizing specific grain boundary structures,

* Corresponding author.
E-mail address: d.raabe@mpie.de (D. Raabe).

http://dx.doi.org/10.1016/j.cossms.2014.06.002
1359-0286/

compositions and properties that enable the design of beneficial material behavior [42–46,58,59]. More specific, GB segregation can be used as a microstructure design method since solutes affect the structure, phase state and atomic bonds within the decorated interface. Different scenarios are conceivable: first, segregation of certain solutes might enhance GB cohesion (GB strengthening). Second, the reverse might apply, namely, reduction in cohesion and bonding strength (interface weakening) at GBs due to segregation. Third, segregation could be strong enough, in conjunction with the available interfacial energy and local stresses, to result in a phase transformation of or at the GB region [58]. Related to the latter point is the possibility for the formation of complexions, i.e., interface stabilized phases [60–66].

An important question in that context is the accessibility of these segregation-dependent GB features via an 'engineering' approach. Indeed various examples are conceivable where such misorientation- and plane-sensitive design approach can work, namely, diffusion annealing, grain growth heat treatment, and local phase transformation effects.

A typical example for an engineering heat treatment approach to tune a desired segregation level at GBs lies in a combined diffusion plus grain growth heat treatment: Since the reduction and GB energy may depend on both, the GB plane inclination and its crystallographic misorientation, such low energy configurations can be obtained for instance by a grain growth heat treatment, where low-energy interfaces prevail owing to their comparably small capillary driving force. Another broadly applicable example of GB segregation engineering lies in the reduction of the average grain size due to an overall drop in GB energy caused by equilibrium segregation.

Although GBSE can be applied to such diverse systems as solar cells [67,68], superconductors [69], or ceramics [60–66] we focus here on recent developments pertaining to metallic alloys used for structural applications [70–82].

In these materials we see particularly high relevance and opportunities of the GBSE concept for designing improved ultra fine grained and nanostructured metallic alloys where GBs constitute a large fraction of the material. Particularly alloys with nanoscaled grain size suffer often from very low ductility in conjunction with inter-crystalline damage. In such materials particularly the internal interfaces are prone to void formation and damage initiation.

Grain boundary segregation: theoretical background and recent experimental progress

Adsorption isotherm

GB segregation is characterized by the inhomogeneous distribution of solutes between the interface and its abutting crystals. The concentration of the solutes on the GB exceeds their solubility in the grain interior, sometimes by a factor of 2–3 and sometimes even by up to several orders of magnitude [40–42]. An approximation for the segregation tendency of a solute is its bulk solubility: the smaller the bulk solubility, the higher is the enrichment factor of that element at the GB. The thermodynamics of GB segregation has close analogy to monolayer gas adsorption at solid surfaces according to Gibbs and can be formalized in terms of the adsorption isotherm [43]. In this concept the GB excess concentration is $\Gamma_i = -1/(RT)(d\gamma/d\ln x_i)_{T,V}$ where x_i are the molar concentrations of the elements i in the bulk, $d\gamma$ is the change in GB energy upon segregation at constant temperature T and volume V. The value for Γ_i can be obtained by measuring the change in interfacial energy as a function of concentration changes in logarithmic presentation.

Although the Gibbs adsorption isotherm outlined above enables a quantitative analysis of GB segregation, the actual measurement of the interfacial energy as a function of bulk composition and temperature is experimentally rather challenging in the case of GBs [16]. Therefore, it is pertinent to use the Langmuir-McLean isotherm [44] which approximates segregation by balancing adsorption and desorption rates. It assumes that dynamic equilibrium is established between the segregating solutes at the GB and that adsorption is limited to one monolayer. The Langmuir-McLean isotherm reads $x_i^{GB}/(x_i^{GB,0} - x_i^{GB}) = x_i^B/(1 - x_i^B)\exp(-\Delta G_i^{GB}/RT)$ where x_i^{GB} is the molar GB occupation fraction of element i, $x_i^{GB,0}$ the molar GB fraction of the same element in saturation, x_i^B is the molar concentration of i in the bulk, and Δx_i^{GB} is the free molar energy of segregation. Approximating the system as a dilute case yields $\beta_i = x_i^{GB}/x_i^B = \exp(-\Delta G_i^{GB}/RT)$ where β_i is the segregation coefficient which is also referred to as GB enrichment factor. The Langmuir-McLean relation states that GB segregation occurs for $\Delta G_i^{GB} < 0$, that GB coverage increases with the bulk solute content and that segregation drops with increasing temperature. The Langmuir-McLean model is usually more practical for quantifying segregation at solid state interfaces than the Gibbs concept, since it does not require detailed knowledge of the GB energy, and its variation with temperature or composition. However, the segregation free energy ΔG_i^{GB} is usually an unknown property. Also, it is worth noting that the Langmuir-McLean segregation model treats the GB implicitly as an individual phase with specific thermodynamic properties, which are different from those of the matrix. Other isotherm models, for instance those by Fowler, Guggenheim and Freundlich, consider interactions among the segregated solutes [46].

Fig. 1 shows experimentally obtained segregation coefficients for a number of Fe-, Ni-, and Cu-matrix binary systems compiled mainly by Hoffmann, Lejček [14,40–42,46], Shea, and Hondros [12,15,39], as well a s some measurements conducted by the current authors using atom probe tomography [29,76,83,85]. Fig. 1 reveals that solutes with very low miscibility, i.e., high positive

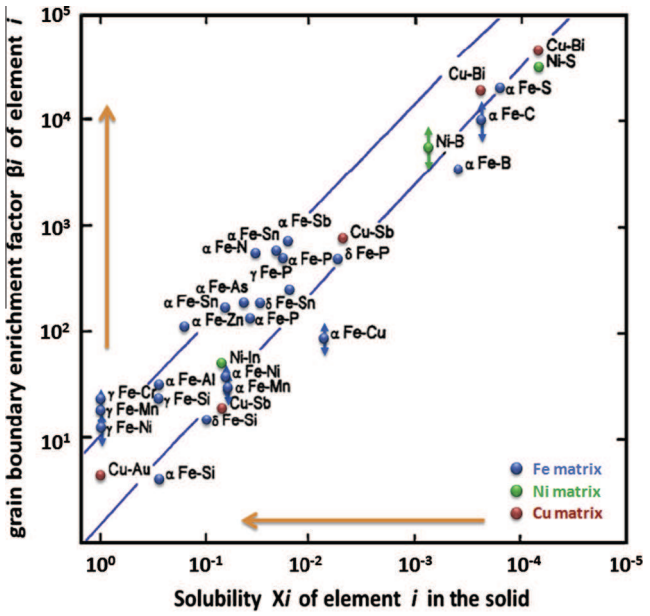

Fig. 1. Grain boundary segregation data compiled from published values of Hoffmann, Lejček [14,40–42,46], Shea, and Hondros [12,15,39], as well as some measurements conducted by the current authors using atom probe tomography [29,76,83,85]. The data show the GB enrichment factor $\beta_i = x_i^{GB}/x_i^B = \exp(-\Delta G_i^{GB}/RT)$ relative to the element's bulk solubility. These data can serve as a guideline for segregation engineering via the identification of suited elements with strong GB segregation tendency.

heat of mixing, segregate strongly. For instance, C in Fe was observed to have a segregation coefficient as large as nearly 10^4.

Recent experimental progress in studying grain boundary segregation, transformation and design

GB segregation can be studied by Auger electron spectroscopy, secondary ion mass spectrometry, transmission electron microscopy, analytical electron microscopy, field ion microscopy and atom probe tomography (APT). While being in principle capable of delivering certain GB segregation information, most of these methods – when used individually – lack either crystallographic detail, chemical resolution, and/or spatial resolution. Also, as there is a large variety of GBs (5 independent crystallographic parameters are required to describe a GB) the achieved statistics are rarely sufficiently robust. Another limitation is that GB segregation data were often taken on embrittled systems, where only those GBs could be probed that were accessible after inter-crystalline fracture, hence, only specific types of GBs could be investigated. Finally, GB segregation is an atomic scale phenomenon, i.e., precise and at the same time statistically significant data are hard to obtain. These principle problems associated with characterizing GB segregation with (a) atomic scale precision and (b) with high crystallographic detail impeded up to now a more quantitative approach to GBSE. This discrepancy between the current theoretical and crystallographic understanding and the accessibility and plausibility of observed and predicted GB segregation effects was recently discussed by Wynblatt and Chatain. They also outlined a model of the dependence of GB segregation on the 5 macroscopic parameters of GB orientation [84].

Further progress along these lines was recently made through the maturation of APT-based and TEM/APT correlative methods [85–96] and by aberration-corrected high resolution analytical TEM techniques [60,61,63,65,97]. The first one is based on lattice reconstruction directly from atom probe data. This approach is also referred to as atom probe crystallography [89–95,86]. The second one is the combination of transmission electron microscopy (TEM) and APT conducted on the same sample position, also referred to as correlative TEM/APT [85–88]. Another method is to obtain crystallographic GB information from EBSD probing on sets of oblique slices (sample edges) in conjunction with subsequent APT probing [96]. These methods are capable of providing complementary characterization of both, atomic scale chemical segregation and the associated crystallography of the GB affected at identical sample positions.

The accuracy of GB segregation data obtained by such correlative mapping methods using electron microscopy (EBSD or TEM) in conjunction with subsequent APT is affected by various factors. First, the angular resolution in the crystallographic characterization of misorientation angles obtained by TEM nanobeam diffraction is typically ~1° [85]. In EBSD it is usually ~1–3° depending on the instrument and software used. Another source of experimental error is the precision of cutting the specimens containing the GB probed portion by FIB. This uncertainty is eliminated if the orientation measurement is directly conducted on the APT tip [85]. This can be done both, by SEM-based EBSD and by TEM nanobeam diffraction, where the latter approach provides high yield and typically also higher orientation precision.

Other errors are associated with APT: first, the allocation of evaporated atoms to a GB (rather than to the abutting grain) depends on projection and lens effects. The projection method is not accessible in current analysis approaches and based on a model of the magnetic field surrounding the tip. Lens effects occur in cases where field evaporation prevails at the decorated GBs leading to distortions of the anticipated ion flight path. In cases of very strong lens effects such positioning errors of the evaporated ions can amount up to several nm.

Another potential source of errors lies in the manual peak fitting of the ladder diagrams, which can be estimated by determining the upper and lower bounds to not exceed ±1 atoms/nm^2 [25,85]. However, all these errors are small compared to the typically measured decoration values as discussed in the following.

To give an example Herbig et al. [85] recently showed that specifically the correlative use of TEM and APT, when applied to investigate GB segregation on nanocrystalline materials containing multiple GBs per APT sample, enables obtaining a high analytical throughput while maintaining excellent spatial and chemical resolution [87]. Fig. 2 shows an example of this approach, applied to

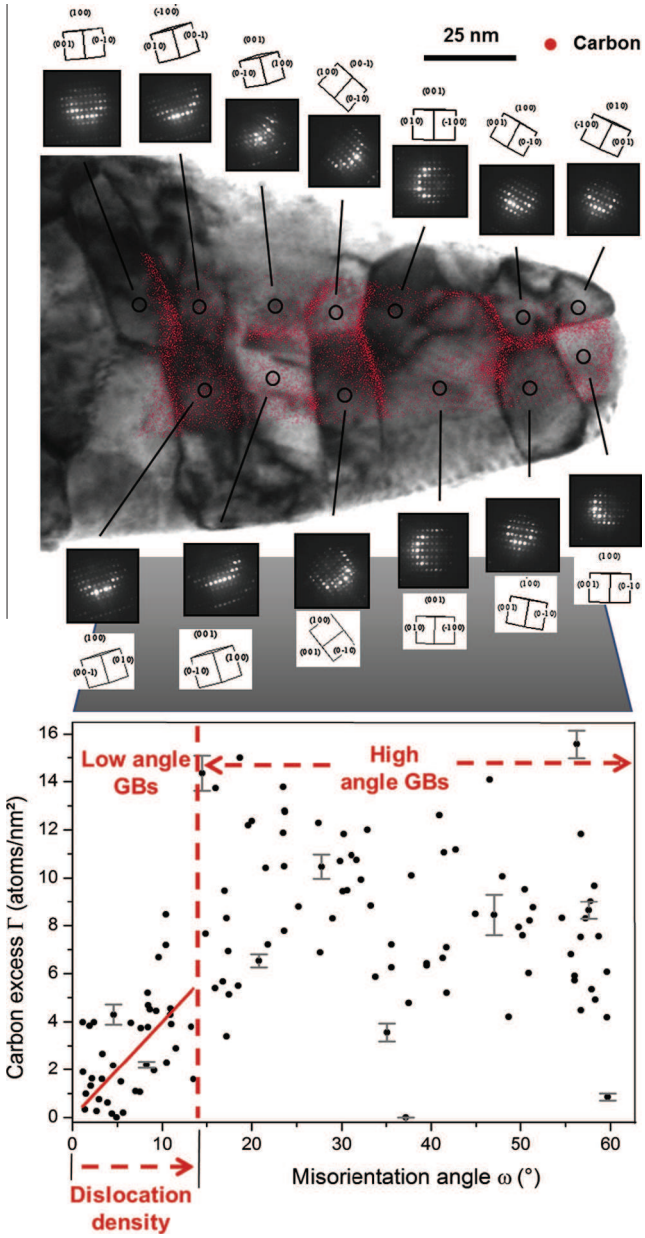

Fig. 2. Advanced method to quantify GB segregation by combined use of TEM and APT on the same sample, here applied to the case of carbon GB segregation in ferrite. Investigating nanocrystalline materials containing multiple GBs per APT sample allows for high throughput while maintaining excellent spatial and chemical resolution [85]. The diagram shows segregation data obtained from 121 GBs on different seven APT tips measured in six days of experimental time. The data are taken from [85].

the characterization of carbon segregation to GBs in a nanocrystalline steel.

Recent progress in simulating GB segregation with respect to segregation engineering

Recent progress in segregation simulations provides opportunities for GBSE. Three developments are emphasized: This is on the one hand the analysis of GB segregation by ab initio simulations [13], in part in close conjunction with corresponding high resolution aberration corrected TEM experiments [98–101]. Duscher et al. [98] studied the origin of catastrophic brittle fracture on the Cu–Bi system. They used a combination of two atomic characterization methods and ab initio simulations to probe the geometric and electronic structure of a Cu GB with and without Bi. The authors mapped the distribution of Bi in the GB plane and further detected thereby induced changes in the electronic structure. The associated density functional theory (DFT) analysis revealed that the Cu atoms surrounding the segregated Bi reduce GB cohesion by assuming a more Zn-like electronic structure. Buban et al. [99] showed via a combined HR-STEM and ab initio study that Zr and Y ions occupy defined segregation sites at alumina GBs and, thereby, influence the GB energy and, consequently, mechanical and electrical properties of alumina. Chen et al. [100] conducted a combined first principle – HR TEM study on the influence of oxygen segregation to 3 and 9 GBs in cubic boron nitride. Their study reveals that oxygen segregation decreases the GB formation energies causing reduced adhesion energies which results in GB weakening. Similarly, Wang et al. [101] showed by using a combination of advanced electron microscopy, spectroscopy and DFT calculations 3D images of complex, multi-component GBs with both atomic resolution and chemical sensitivity. They observed that even a simple MgO compound revealed complex ordered defect superstructures on its GBs inducing electron trapping in the band-gap of the oxide. While DFT based simulation methods offer certainly the most precise results and deep insight into bonding effects due to segregation, they are typically confined to analyzing high symmetry interfaces with a low CSL value. This is due to the fact that DFT solvers require the use of periodic boundary conditions. Also, important progress is stimulated by using molecular dynamics and molecular statics simulations in conjunction with improved interatomic potentials that are in part based on DFT simulations [102]. In this context specifically bonding effects stemming from the magnetic moments are challenging to capture in systems based on Fe-, Co-, or Ni [103]. Atomic scale simulations, although providing less electronic detail compared to first principles predictions, offer the advantage to study also less ordered GBs. Important applications of such simulations towards GBSE can be seen in simulation on the topic of grain size stabilization in nanocrystalline materials [17,104,105] owing to the segregation-driven reduction in GB energy [22,23,43,105].

At a more coarse grained level, beyond vibrational modes, phase field and phase field crystal modeling can be used as an alternative to predict interactions of mechanical and chemical phenomena at the single GB scale [107,108]. In the context of GBSE the phase field model has recently been used for instance to predict solute decoration and phase transformation phenomena at segregation decorated GBs [58,109–111].

From GB segregation to GB segregation engineering: Examples

Alloy design by applying GB segregation engineering

An important field where GBSE is used for improving material performance is the B doping of creep resistant polycrystalline Ni-based alloys used for power plant applications at temperature of up to 700 °C. Fig. 3 shows an example of alloy 617 where B segregation on high angle GBs was revealed by using correlative TEM and APT, leading to enhanced GB cohesion and the promotion of the formation of precipitates [78].

Another domain where GBSE can be efficiently employed is the stabilization of nano-crystalline grains [17,104,105] by reducing the GB energy through segregation, Fig. 4 [22,23,43,105]. Many nanocrystalline metallic materials undergo undesired discontinuous grain growth already at modest temperatures owing to the high capillary driving pressure exerted through the interfacial energy. Hence, inserting solute segregation to GBs in such systems is an essential target for two reasons: firstly, the capillary driving force for competitive grain coarsening is reduced and secondly, when choosing adequate solutes, GB cohesion can be enhanced. In some systems this principle was successfully used to stabilize nanocrystalline structures [112–121]. Recently it was observed that C decoration to GBs is an essential principle behind the stabilization of nanocrystalline grains and sub-grains and its resulting effects on the strength of heavily deformed pearlitic steel wires [75,76,122,123] and martensite [71].

Alloy design by using segregation-driven GB phase transformation

The concept of GBSE can be developed further by combining GB segregation with elastic stresses to promote local phase transformation at GBs [29,58]. This effect was observed at GBs in high strength steels and in Ti alloys. It works specifically for segregation in conjunction with subsequent martensite-to-austenite reversion at martensite GBs. These transformed interface regions can act as compliance layers or, respectively, mechanical buffer zones impeding for instance crack penetration along lath martensite lamellae. Also, such regions can facilitate further phase transformation and hence larger austenite zones which can initiate a nano-scale TRIP effect (transformation induced plasticity) [29,58,59]. Martensite reveals rather different types of GBs, namely, prior austenite, packet, block, or lath boundaries, which have all different energy, structure, misorientation, mechanics, and segregation properties [124–127] and which could in principle all be manipulated in the way described.

These results reveal that the approach of reversing martensite GBs back into austenite via GB segregation is a very efficient way of making the material more resistant against crack penetration. Specifically, in martensite lath structures with their low mutual misorientations, a thin austenite buffer layer, impeding crack penetration, is of specific benefit. In order to realize local phase transformations of martensite lath GBs at modest heat treatments a set of criteria has been suggested [29,58,59]: First, elements with a high segregation coefficient should be chosen. Second, these elements should reduce the transformation temperature from martensite to austenite. Third, they should prefer segregation over bulk precipitation (e.g., carbide formation). Fourth, nucleation should be supported in the GB region e.g., by elastic stresses.

Complexions

In classical interface theories the existence of three types of GB phases is discussed: These are intrinsic (undecorated) GBs; monolayer adsorption layers; and GB wetting films. However, recent TEM work revealed the existence of further types of impurity-containing intergranular films of equilibrium thickness in various ceramics and metals, as well as at metal-ceramic hetero-interfaces. Dillon, Harmer, Cantwell et al. [61–66] and Baram et al. [60] formulated an extension of the Gibbs definition of a bulk phase to interfacial features. They refer to these equilibrium states as interface complexions. More specifically, the concept suggests that such

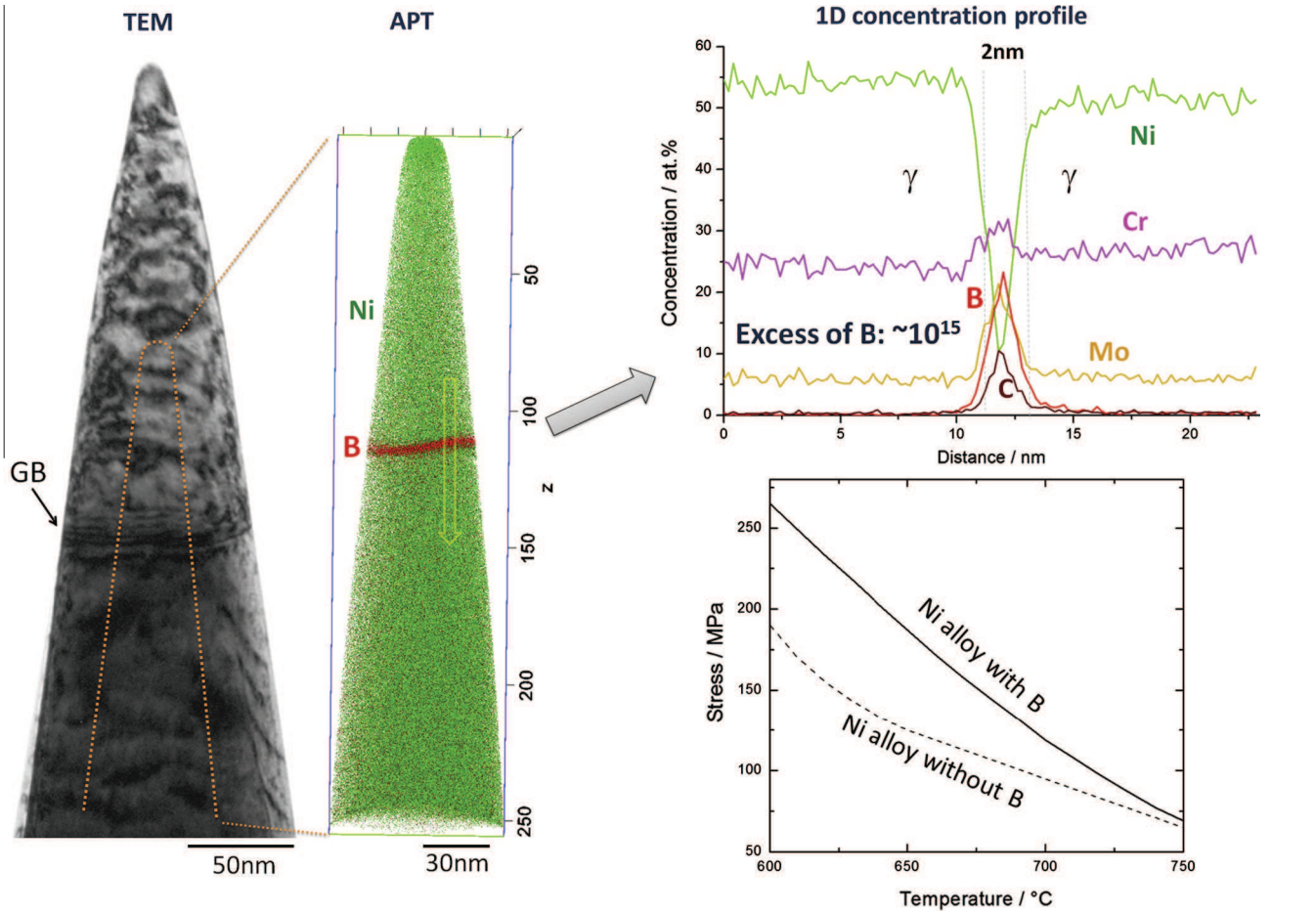

Fig. 3. Segregation of B to a high angle GB in Ni-alloy 617. B improves – via improved GB cohesion and GB precipitation – the rupture strength as shown in terms of the comparison of alloy 617 (Nicrofer5520Co) and the B-doped variant alloy 617B (Nicrofer5520CoB) in the range between 600 and 750 °C (10^5h). Data taken from [78].

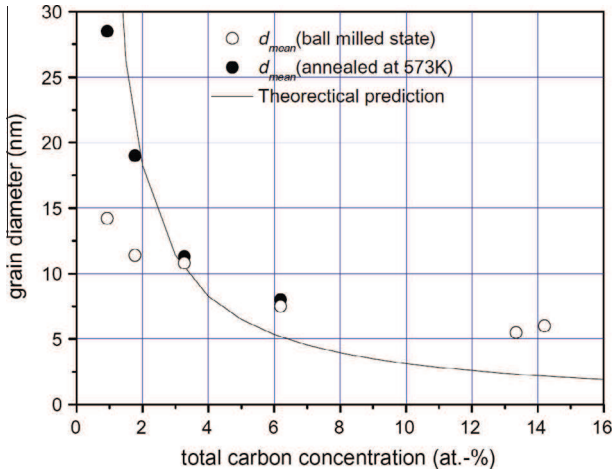

Fig. 4. Dependence of the average grain diameter, d_{mean}, on the total carbon concentration in a ball-milled Fe–C alloy. The diagram is taken from the work of Chen et al. [106].

complexions are interface-stabilized phases (also referred to as interphases) that are chemically and structurally distinct from any of the abutting bulk phases. Baram et al. [60] studied such effects on interface structures between gold and metal oxide. They found that the interface structures formed equilibrium phases that obey thermodynamic rules analogous to those applied to bulk phases. They suggest that an interface complexion can be considered as a separate interface phase, which can transform into different other phases (complexions) with different properties by adjusting chemistry and heat treatment. Dillon et al. [62] studied this phenomenon on alumina with controlled doping of impurities. High-resolution TEM revealed that GBs could either consist of one chemical species; have a single adsorbed (segregated) monolayer of a solute; an adsorbed bilayer of one or more solutes; multiple adsorbed layers; or thin intergranular wetting films of constant thickness. It was also observed that transitions from one complexion to another can be accompanied by a reduction in energy. From these observations the authors suggested that bulk phase diagrams can be modified to include equilibrium interface phases, or complexions [60].

The thermodynamic stability of these nanoscale impurity-containing intergranular films was explained in terms of a balance of various interfacial forces and by making analogies to surface pre-melting and pre-wetting theories. If GBs and surface adsorptions are analogous, one may also expect that, in certain systems, interfacial phases can take on a discrete thickness, leading to the formation of distinct bilayer and trilayer interfacial phases [60,128].

These observations on complexions are conceived to be relevant to the field of GB segregation engineering, and hence, included here. It should be noted that the level of solute segregation is – like temperature – a variable that determines the state and energy of a GB that can be relatively easy and effectively manipulated. It can be assumed that segregation and subsequent possible phase formation at a decorated GB might proceed via a sequence of GB

phase states before finally a new bulk phase is formed at the decorated GB.

Both, the sequence and the final GB state depend on the corresponding free energy ratios among the competing phases. Hence, by picking adequate alloying elements or combinations of them, solute decoration vs. phase transformation or respectively complexion formation can be designed and guided provided that corresponding free energy data are available.

Improving interface damage resistance via GB segregation engineering

Here we discuss as an example a set of experiments on temper embrittlement of a binary Fe–8.8 wt.% Mn alloy. The aim is to reflect on the possible effects of GB segregation engineering on the material's resistance to crack formation, crack propagation, and failure. The model alloy discussed here for this purpose was after quenching subjected to a diffusion heat treatment at 450 °C for different annealing times ranging from a few minutes to several 100 h. The damage resistance of the heat treated samples was then studied by impact tests, Fig. 5. The mechanical analysis was accompanied by microstructural investigations of the GBs after the different heat treatment intervals.

The data reveal a strong and non-linear dependence of the observed impact energy, used here as a measure for the materials toughness, on the heat treatment duration. For short annealing times at 450 °C in the range between a few seconds and up to 100 h the alloy undergoes a substantial embrittlement where it practically loses all of its toughness. For very long annealing times beyond several 100 h at this temperature the alloy does not only recover most of its original toughness observed after quenching but even shows higher values than it originally had.

Although these data were not obtained by fatigue testing it may be anticipated that this trend of the embrittlement as a function of heat treatment time may be applicable also to other loading states rather than the here imposed impact testing.

The primary reason for the immediate embrittlement of the alloy already after very short annealing times at 450 °C is attributed to the segregation of Mn to the GBs and the associated decohesion that it causes. The recovery in toughness, however, observed for very long annealing times, is less well understood at this stage. Two explanations can be put forward in this context. The first one refers to the effect of very high Mn segregation to the GBs and the associated martensite to austenite reverse transformation [29,58]. This would lead to thin austenitic layers between the martensitic laths which might act as a soft barrier against crack propagation. Similar effects are discussed for Ti alloys where thin films of β-Ti, located between α-Ti crystals, might play a similar role. The here assumed blunting effect on cracks when entering into such soft GB phase layers is, however, still under debate.

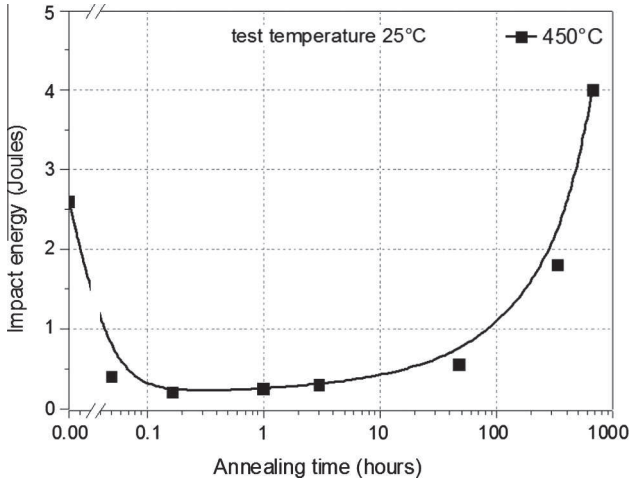

Fig. 5. Influence of Mn segregation on the development of the toughness of a Fe–8.8 wt.% Mn alloy after different annealing times at 450 °C.

The second effect refers also to the formation of reversed austenitic zones on the martensite GBs. However, the underlying effect that is here assumed to increase GB cohesion with increasing annealing time lies in the 'cleaning' effect that the formation and growth of these austenite islands have. The idea is that once an austenitic nucleus is formed on a martensitic GB, partitioning leads to the accumulation of Mn into this newly formed austenite film, thus removing solute Mn from the martensite GB. Hence, less Mn segregates to the martensite GBs, recovering some of the original GB cohesion. Also this effect has still to be analyzed in more detail.

Another more trivial additional reason for improving damage resistance of alloys due to GB segregation engineering lies in the reduction of the GB energy due to equilibrium solute decoration according to the Gibbs adsorption isotherm. This means that during heat treatments the driving force for capillary-driven grain coarsening is reduced, leading to an overall smaller grain size.

Current challenges and opportunities in GB segregation engineering

A specific challenge in GB research and, more specifically, in the field of GB engineering related to segregation (GBSE), lies in the joint characterization of both, structure and chemistry of GBs at atomic scale. The difficulty lies in the multiple degrees of freedom associated with the description of a GB (5 crystallographic and 3 atomistic parameters) that all affect GB segregation. This results in an almost infinite amount of GB variants which renders the identification of correlations between GB type and segregation and the associated investigation of manipulation opportunities challenging [85,129–131]. Even the often helpful simplification of this problem into three GB classes, namely, low angle GBs, random high angle GBs, and highly coherent GBs, is not generally useful in this context. This is due to the fact that in the field of GBSE even the most coherent GBs, i.e., twin boundaries, can contain incoherent portions, typically in the form of ledges or facets that deviate from coherency where impurities reside and locally alter the GB's properties. In other words, approaches towards GBSE cannot be based merely on the CSL concept but may have to consider the GB plane inclination or GB defect structures, too [85]. Very similar arguments hold for corresponding ab initio, MD, or phase field crystal simulations.

It should be emphasized that in some cases a simplifying GBSE approach is conceivable though. For instance when aiming at reducing the overall grain size by segregation engineering, leading to the reduction in the grain boundary energy and mobility, a global trend information about the degree of equilibrium solute decoration of non-ordered or 'random' GBs is sufficient. Hence, in such cases a 5D crystallographic analysis of segregation is not necessarily required but instead the overall level of solute partitioning between grain interiors and the abutting GBs suffices as starting information for a GBSE approach, using for instance segregation trends as presented in Fig. 1. Also, in systems with a high fraction of low angle GBs, such as for instance observed in subgrain structures in aluminum alloys and low carbon steels, a nearly linear trend between the misorientation and the solute decoration was observed, Fig. 2. Hence, also in such cases the GBSE approach does not require a full 5D GB analysis, i.e., GB planes can be neglected in a first approach.

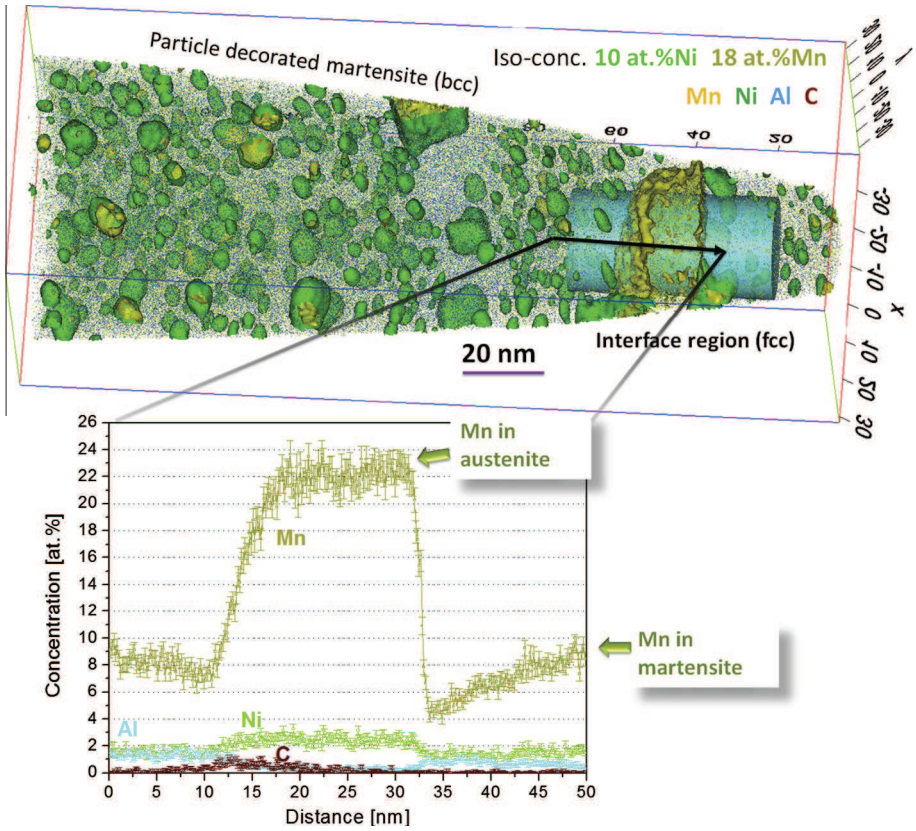

Fig. 6. Formation of a 15 nm thick film of reversed austenite and the associated Mn partitioning at a former martensite GB after tempering at 450 °C for 48 h. The martensitic regions are decorated with spherical precipitates. The alloy is a Fe–9Mn–1.9Ni–0.6Mo–1.1Ti–0.33Al–0.1Si–0.05C (at.%) maraging steel. Data are taken from [58].

Another opportunity to overcome the enormous challenges associated with conducting experiments in such a huge parameter space lies in using corresponding simulation methods which enable chemical trend screening of GB decoration. While density functional theory is not an adequate method for such trend screens owing to the requirement of using periodic boundary conditions and small simulation cells, the phase field crystal model might be suited to systematically tackle such a task [132,133]. The phase field crystal method is a quasi-continuum model that works at atomic length and diffusive time scales assuming conservative dynamics. It can be informed by atomic interactions obtained from density functional theory. The phase field crystal method can treat the overdamped dynamics of several 10^7 atoms.

Applications where GBSE could help to improve material performance are the fields of GB oxidation, cohesion, damage, GB-assisted phase transformation, and creep pore formation. In the case of oxidation, segregation alters the local chemical state and creates a local potential difference between the GB and the abutting bulk crystals. This mechanism can lead to faster local oxidation at GBs which is an effect that is amendable to GBSE. Cohesion at GBs can be influenced by segregating solutes that increase rather than decrease cohesion. An example of B segregation in Ni was given in Fig. 3. Also, the co-segregation of beneficial, cohesive solutes to GBs can be an interesting strategy to occupy atomic positions at GBs with the aim to avoid segregation of solutes that reduce cohesion. Finally, the formation of compliant phases (Fig. 6) or suited segregation occupation at GBs can prevent damage initiation, for instance by arresting cracks at GBs. These locally formed GB phases do not necessarily have to be complexions, i.e., interface stabilized phases, but can be conventional phases that preferentially form at decorated GBs. Examples are the formation of austenite at martensite GBs or the formation of β-Ti films at former α-Ti GBs.

Conclusions and outlook

Recent theoretical and experimental advances in the fields of GB segregation and GB phase transformations offer opportunities for the manipulation of internal interfaces with the aim of improving the materials' mechanical response. Although the focus was placed here on metallic alloys, similar principles apply to ceramic materials and semiconductors. Solute decorated GBs can lead to different types of equilibrium phenomena. These include classical equilibrium segregation; monolayer occupation; bi- and trilayer occupation (i.e., complexions, interface stabilized phases); wetting; and regular equilibrium bulk phase formation or, respectively, phase reversion. All these types of segregation-induced GB phenomena can be utilized to design specific features for improving the mechanical response of such alloys. Examples are the increase in GB cohesion, fracture toughness, or resistance against creep pore formation. We refer to this approach of manipulating GBs by solute decoration and phase transformations as grain boundary segregation engineering.

References

[1] McLean D. Grain boundaries in metals. London: Oxford Press; 1957.
[2] Sutton AP, Ballufi RW. Interfaces in crystalline materials. USA: Oxford University Press; 1997.
[3] Randle V. The measurement of grain boundary geometry. Bristol: Taylor and Francis; 1993.
[4] Howe JM. Interfaces in materials: atomic structure, thermodynamic and kinetics of solid–vapor, solid–liquid and solid–solid interfaces. New York: Wiley; 1997.
[5] Rollet AD, Gottstein G, Shvindlerman LS, Molodov DA. Grain boundary mobility – a brief review. Z Metallkd 2004;95:226–9.
[6] Wolf, D. Atomic-level geometry of crystalline interfaces, in: Materials interfaces: atomic-level structure and properties, Chapman & Hall, London, 1992.

[7] Gottstein G, Shvindlerman LS. Grain boundary migration in metals – thermodynamics, kinetics. Boca Raton: Applications. CRC Press; 1999.
[8] Watanabe T, Kitamure S, Karashima S. Grain boundary hardening and segregation in alpha Iron-Tin alloy. Acta Metall 1980;28:455–63.
[9] Watanabe T, Tsurekawa S. The control of brittleness and development of desirable mechanical properties in polycrystalline systems by grain boundary engineering. Acta Mater 1999;47:4171–85.
[10] Randle V. Twinning-related grain boundary engineering. Acta Mater 2004;52:4067–81.
[11] Randle V. Mechanism of twinning-induced grain boundary engineering in low stacking-fault energy materials. Acta Mater 1999;47:4187–96.
[12] Shea MP. Interface adsorption, embrittlement and fracture in metallurgy: a review. Surf Sci 1975;53:168–212.
[13] Wu R, Freeman AJ, Olson GB. First principles determination of the effects of phosphorus and boron on iron grain boundary cohesion. Science 1994;15:376–80.
[14] Lejček P, Hofmann S, Paidar V. Segregation based classification of [100] tilt grain boundaries in α-iron and its consequences for grain boundary engineering. Acta Mater 2003;51:3951–63.
[15] Seah MP, Hondros ED. Grain boundary segregation. Proc R Soc London. Ser A, Math a, Phys Sci 1973:191–212.
[16] Defay R, Prigogine I. Surface tension of regular solutions. T Faraday Soc 1950;46:199–204.
[17] Millett PC, Selvam RP, Saxena A. Molecular dynamics simulations of grain size stabilization in nanocrystalline materials by addition of dopants. Acta Mater 2006;54:297–303.
[18] Millett PC, Selvam RP, Saxena A. Stabilizing nanocrystalline materials with dopants. Acta Mater 2007;55:2329–36.
[19] Hondros ED. The influence of phosphorus in dilute solid solution on the absolute surface and grain boundary energies of iron. Proc R Soc London A 1965;286:479–98.
[20] Wynblatt PW, Chatain D. Anisotropy of segregation at grain boundaries and surfaces. Metall Mater Trans A 2006;37:2595–620.
[21] Jiang H, Faulkner RG. Modelling of grain boundary segregation, precipitation and precipitate-free zones of high strength aluminium alloys – I. The model. Acta Mater 1996;44:1857–64.
[22] Kirchheim R. Grain coarsening inhibited by solute segregation. Acta Mater 2002;50:413–9.
[23] Kirchheim R. Reducing grain boundary, dislocation line and vacancy formation energies by solute segregation. I: Theoretical background. Acta Mater 2007;55:5129–38.
[24] Lozano-Perez S, Saxey DW, Yamada T, Terachi T. Atom-probe tomography characterization of the oxidation of stainless steel. Scr Mater 2010;62:855–8.
[25] Ohsaki S, Raabe D, Hono K. Mechanical alloying and amorphization in Cu–Nb–Ag in situ composite wires studied by transmission electron microscopy and tomographic atom probe. Acta Mater 2009;57:5254–63.
[26] Mattissen D, Raabe D, Heringhaus F. Experimental investigation and modeling of the influence of microstructure on the resistive conductivity of a Cu–Ag–Nb in situ composite. Acta Mater 1999;47:1627–34.
[27] Herzig C, Divinski SV. Grain boundary diffusion in metals: recent developments. Mater Trans 2003;44:14–27.
[28] Duarte MJ, Klemm J, Klemm SO, Mayrhofer KJJ, Stratmann M, Borodin S, et al. Element-resolved corrosion analysis of stainless-type glass-forming steels. Science 2013;341:372–6.
[29] Dmitrieva O, Ponge D, Inden G, Millán J, Choi P, Sietsma J, et al. Chemical gradients across phase boundaries between martensite and austenite in steel studied by atom probe tomography and simulation. Acta Mater 2011;59:364–74.
[30] Koyama M, Akiyama E, Sawaguchi T, Raabe D, Tsuzaki K. Hydrogen-induced cracking at grain and twin boundaries in an Fe–Mn–C austenitic steel. Scr Mater 2012;66:459–62.
[31] Koyama M, Akiyama E, Tsuzaki K, Raabe D. Hydrogen-assisted failure in a twinning-induced plasticity steel studied under in situ hydrogen charging by electron channeling contrast imaging. Acta Mater 2013;61:4607–18.
[32] Cahn JW. The impurity-drag effect in grain boundary motion. Acta Metall 1962;10:789–98.
[33] Lücke K, Detert K. A quantitative theory of grain-boundary motion and recrystallization in metals in the presence of impurities. Acta Metall 1957;5:628–37.
[34] Molodov DA. In: Gottstein G, Molodov DA, editors. Grain boundary character – a key factor for grain boundary control. Recrystallization and grain growth, vol. 1. Aachen: Springer Verlag; 2001. p. 21–38.
[35] Winning M, Gottstein G, Shvindlerman LS. On the mechanisms of grain boundary migration. Acta Mater 2002;50:353–63.
[36] Czubayko U, Molodov DA, Petersen BC, Gottstein G, Shvindlerman LS. An X-ray device for continuous tracking of moving interfaces in crystalline solids. Mater Sci Technol 1995;6:947–52.
[37] Furtkamp M, Gottstein G, Molodov DA, Semenov VN, Shvindlerman LS. Grain boundary migration in Fe–3.5% Si bicrystals with [001] tilt boundaries. Acta Mater 1998;46:4103–10.
[38] Gottstein G, Shvindlerman LS, Molodov DA, Czubayko U. Grain boundary motion in aluminium bicrystals. In: Duxbury PM, Pence TJ (editors). Dynamics of crystal surfaces and interfaces, New York: Plenum Press; 1997. P. 109–23.
[39] Hondros ED, Seah MP. The theory of grain boundary segregation in terms of surface adsorption analogues. Metall Trans 1977;8A:1363–71.
[40] Hoffman S. Segregation of grain boundaries. In: Dowben PA, Miller A, editors. Surface segregation phenomena. Boca Raton: CRC Press; 1990. p. 107–1134.
[41] Hoffman S, Lejcek P. Solute segregation at grain boundaries. Interface Sci 1996;3:241–67.
[42] Lejcek P, Hoffman S. Thermodynamics of grain boundary segregation and applications to anisotropy, compensation effect and prediction. Crit Rev Solid State 2008;33:133–63.
[43] Gibbs JW. The Collected Works of J. Willard Gibbs, Vol. 1, Yale University Press, New Haven, CT, 1948.
[44] Langmuir I. The adsorption of gases on plane surfaces of glass mica and platinum. J Am Chem Soc 1918;40:1361–8.
[45] Liu F, Kirchheim R. Grain boundary saturation and grain growth. Scr Mater 2004;51:521–5.
[46] Lejček P, Hofmann S. Thermodynamics and structural aspects of grain boundary segregation. Crit Rev Solid State 1995;20:1–85.
[47] Chapman MAV, Faulkner RG. Computer modelling of grain boundary segregation. Acta Metall 1983;31:677–89.
[48] Livingston JD, Chalmers B. Multiple slip in bicrystal deformation. Acta Metall 1957;5:322–7.
[49] Shen Z, Wagoner RH, Clark WAT. Dislocation pile-up and grain boundary interactions in 304 stainless steel. Scr Metall 1986;20:921–6.
[50] Bamford TA, Hardiman B, Shen Z, Clark WAT, Wagoner RH. Micromechanism of slip propagation through a high angle boundary in alpha brass. Scr Metall 1986;20:253–8.
[51] Lee TC, Robertson IM, Birnbaum HK. Prediction of slip transfer mechanisms across grain boundaries. Scr Metall 1989;23:799–803.
[52] Lee TC, Robertson IM, Birnbaum HK. An in situ transmission electron microscopy deformation study of the slip transfer mechanisms in metals. Metall Trans A 1990;21:2437–47.
[53] Lee TC, Robertson IM, Birnbaum HK. TEM in situ deformation study of the interaction of lattice dislocation with grain boundaries in metals. Philos Magn A 1990;62:131–53.
[54] Clark WAT, Wagoner RH, Shen ZY, Lee TC, Robertson IM, Birnbaum HK. On the criteria for slip transmission across interfaces in polycrystals. Script Metall Mater 1992;26:203–6.
[55] Ma A, Roters F, Raabe D. On the consideration of interactions between dislocations and grain boundaries in crystal plasticity finite element modeling – theory, experiments, and simulations. Acta Mater 2006;54:2181–94.
[56] Ma A, Roters F, Raabe D. Studying the effect of grain boundaries in dislocation density based crystal plasticity finite element simulations. Int J Solids Struct 2006;43:7287–303.
[57] Bieler TR, Eisenlohr P, Roters F, Kumar D, Mason DE, Crimp MA, et al. The role of heterogeneous deformation on damage nucleation at grain boundaries in single phase metals. Int J Plasticity 2009;25:1655–83.
[58] Raabe D, Sandlöbes S, Millán J, Ponge D, Assadi H, Herbig M, et al. Segregation engineering enables nanoscale martensite to austenite phase transformation at grain boundaries: a pathway to ductile martensite. Acta Mater 2013;61:6132–52.
[59] Raabe D, Ponge D, Dmitrieva O, Sander B. Nano-precipitate hardened 1.5 GPa steels with unexpected high ductility. Scr Mater 2009;60:1141–4.
[60] Baram M, Chatain D, Kaplan WD. Nanometer-thick equilibrium films: the interface between thermodynamics and atomistics. Science 2011;332:206–9.
[61] Dillon SJ, Harmer MP. Multiple grain boundary transitions in ceramics: a case study of alumina. Acta Mater 2007;55:5247–54.
[62] Dillon SJ, Harmer MP, Rohrer GS. The relative energies of normally and abnormally growing grain boundaries in alumina displaying different complexions. J Am Ceram Soc 2010;93:1796–802.
[63] Dillon SJ, Harmer MP. Direct observation of multilayer adsorption on alumina grain boundaries. J Am Ceram Soc 2007;90:996–8.
[64] Dillon SJ, Tang M, Carter WC, Harmer MP. Complexion: a new concept for kinetic engineering in materials science. Acta Mater 2007;55:6208–18.
[65] Harmer MP. The phase behavior of interfaces. Science 2011;332:182–3.
[66] Cantwell PR, Tang M, Dillon SJ, Luo J, Rohrer GS, Harmer MP. Grain boundary complexions. Acta Mater 2014;62:1–48.
[67] Choi PP, Cojocaru-Miredin O, Wuerz R, Raabe D. Comparative atom probe study of Cu(In, Ga)Se(2) thin-film solar cells deposited on soda-lime glass and mild steel substrates. J Appl Phys 2012;110:124513.
[68] Cojocaru-Miredin O, Choi PP, Wuerz R, Raabe D. Exploring the p-n junction region in Cu(In, Ga)Se-2 thin-film solar cells at the nanometer-scale. Appl Phys Lett 2012;101:181603.
[69] Sandim MJR, Tytko D, Kostka A, Choi PP, Awaji S, Watanabe K, et al. Grain boundary segregation in a bronze-route Nb3Sn superconducting wire studied by atom probe tomography. Supercond Sci Technol 2013;26:055008.
[70] Thuillier O, Danoix F, Goné M, Blavette D. Atom probe tomography of the austenite–ferrite interphase boundary composition in a model alloy Fe–C–Mn. Scr Mater 2006;55:1071–4.
[71] Yuan L, Ponge D, Wittig J, Choi P, Jiminez JA, Raabe D. Nanoscale austenite reversion through partitioning, segregation and kinetic freezing: example of a ductile 2 GPa Fe–Cr–C steel. Acta Mater 2012;60:2790–804.
[72] Danoix F, Julien D, Sauvage X, Copreaux J. Direct evidence of cementite dissolution in drawn pearlitic steels observed by tomographic atom probe. J Mater Sci Eng A 1998;250:8–13.
[73] Sauvage X, Copreaux J, Danoix F, Blavette D. Atomic-scale observation and modelling of cementite dissolution in heavily deformed pearlitic steels. Philos Magn A 2000;80:781–96.

[74] Hono K, Ohnuma M, Murayama M, Nishida S, Yoshie A. Cementite decomposition in heavily drawn pearlite steel wire. Scr Mater 2001;44:977–83.
[75] Li YJ, Choi PP, Borchers C, Westerkamp S, Goto S, Raabe D, et al. Atomic-scale mechanisms of deformation-induced cementite decomposition in pearlite. Acta Mater 2011;59:3965–77.
[76] Li YJ, Choi PP, Goto S, Borchers C, Raabe D, Kirchheim R. Evolution of strength and microstructure during annealing of heavily cold-drawn 6.3 GPa hypereutectoid pearlitic steel wire. Acta Mater 2012;60:4005–16.
[77] Sangid MD, Sehitoglu H, Maier HJ, Niendorf T. Grain boundary characterization and energetics of superalloys. Mater Sci Eng A 2010;527:7115–25.
[78] Tytko D, Choi PP, Klöwer J, Kostka A, Inden G, Raabe D. Microstructural evolution of a Ni-based superalloy (617B) at 700 °C studied by electron microscopy and atom probe tomography. Acta Mater 2012;60:1731–40.
[79] Prokoshkina D, Esin VA, Wilde G, Divinski SV. Grain boundary width, energy and self-diffusion in nickel: effect of material purity. Acta Mater 2013;61:5188–97.
[80] Abuzaid W, Sangid MD, Carroll J, Sehitoglu H, Lambros J. Slip transfer and plastic strain accumulation across grain boundaries in Hastelloy X. J Mech Phys Solids 2012;60:1201–20.
[81] Pradeep KG, Wanderka N, Choi PP, Banhart J, Murty BS, Raabe D. Atomic-scale compositional characterization of a nanocrystalline AlCrCuFeNiZn high-entropy alloy using atom probe tomography. Acta Mater 2013;61:4696–706.
[82] Singh S, Wanderka N, Murty BS, Glatzel U, Banhart J. Decomposition in multi-component AlCoCrCuFeNi high-entropy alloy. Acta Mater 2011;59:182–90.
[83] Dmitrieva O, Ponge D, Inden G, Millán J, Choi PP, Sietsma J, et al. Chemical gradients across phase boundaries between martensite and austenite in steel studied by atom probe tomography and simulation. Acta Mater 2011;59:364–74.
[84] Wynblatt P, Chatain D. Anisotropy of segregation at grain boundaries and surfaces. Metall Mater Trans A 2006;37:2595–620.
[85] Herbig M, Raabe D, Li YJ, Choi P, Zaefferer S, Goto S. Atomic-scale quantification of grain boundary segregation in nanocrystalline material. Phys Rev Lett 2014;112:126103.
[86] Felfer PJ, Alam T, Ringer SP, Cairney JM. A reproducible method for damage-free site-specific preparation of atom probe tips from interfaces. Microsc Res Techniq 2012;75:484–91.
[87] Krakauer BW, Hu JG, Kuo SM, Mallick RL, Seki A, Seidman DN, et al. A system for systematically preparing atomprobe fieldion microscope specimens for the study of internal interfaces. Rev Sci Instrum 1990;61:3390–8.
[88] Toji Y, Matsuda H, Herbig M, Choi PP, Raabe D. Atomic-scale analysis of carbon partitioning between martensite and austenite by atom probe tomography and correlative transmission electron microscopy. Acta Mater 2014;65:215–28.
[89] Gault B, Moody MP, Cairney JM, Ringer SP. Atom probe crystallography. Mater Today 2012;15:378–86.
[90] Araullo-Peters VJ, Gault B, Shrestha SL, Yao L, Moody MP, Ringer SP, et al. Atom probe crystallography: atomic-scale 3-D orientation mapping. Scr Mater 2012;66:907–10.
[91] Moody MP, Tang F, Gault B, Ringer SP, Cairney JM. Atom probe crystallography: characterization of grain boundary orientation relationships in nanocrystalline aluminium. Ultramicroscopy 2011;111(2011):493–9.
[92] Kelly TF, Larson DJ. Atom probe tomography. Annu Rev Mater Res 2012;42:1–31.
[93] Moody MP, Gault B, Stephenson LT, Haley D, Ringer SP. Qualification of the tomographic reconstruction in atom probe by advanced spatial distribution map techniques. Ultramicroscopy 2009;109:815–24.
[94] Vurpillot F, Cerezo A, Blavette D, Larson DJ. Modeling image distortions in 3DAP. Microsc Microanal 2004;10:384–90.
[95] Liddicoat PV, Liao XZ, Zhao YH, Zhu YT, Murashkin MY, Lavernia EJ, et al. Nanostructural hierarchy increases the strength of aluminium alloys. Nat Commun 2010;63:1–7.
[96] Mandal S, Pradeep KG, Zaefferer SD, Raabe D. A novel approach to measure grain boundary segregation in bulk polycrystalline materials in dependence of the boundaries' five rotational degrees of freedom, Scr Mater, (Available 20.02.14).
[97] Yu ZY, Wu Q, Rickman JM, Chan HM, Harmer MP. Atomic-resolution observation of Hf-doped alumina grain boundaries. Scr Mater 2013;68:703–6.
[98] Duscher G, Chisholm MF, Alber U, Ruhle M. Bismuth-induced embrittlement of copper grain boundaries. Nat Mater 2004;3:621–6.
[99] Buban JP, Mizoguchi T, Shibata N, Abe E, Yamamoto T, Ikuhara Y. Zr segregation and associated Al vacancies in alumina grain boundaries. J Ceram Soc Jpn 2011;119:840–4.
[100] Chen C, Lv S, Wang Z, Saito M, Shibata N, Taniguchi T, et al. Oxygen segregation at coherent grain boundaries of cubic boron nitride. Appl Phys Lett 2013;102:091607.
[101] Wang ZC, Saito M, McKenna KP, Gu L, Tsukimoto S, Shluger AL, et al. Atom-resolved imaging of ordered defect superstructures at individual grain boundaries. Nat Mater 2011;479:380–3.
[102] Ackland GJ, Mendelev MI, Srolovitz DJ, Han S, Barashev AV. Development of an interatomic potential for phosphorus impurities in alpha-iron. J Phys Condens Mater 2014;16:S2629–42.
[103] Mrovec M, Nguyen-Manh D, Elsässer C, Gumbsch P. Magnetic bond-order potential for iron. Phys Rev Lett 2014;106:246402.
[104] Tschopp MA, Solanki KN, Gao F, Sun X, Khaleel MA, Horstemeyer MF. Probing grain boundary sink strength at the nanoscale: energetics and length scales of vacancy and interstitial absorption by grain boundaries in alpha-Fe. Phys Rev B 2012;85:064108.
[105] Detor AJ, Schuh CA. Grain boundary segregation, chemical ordering and stability of nanocrystalline alloys: atomistic computer simulations in the Ni–W system. Acta Mater 2007;55:4221–32.
[106] Chen YZ, Herz A, Li YJ, Borchers C, Choi PP, Raabe D, Kirchheim R. Nanocrystalline Fe–C alloys produced by ball milling of iron and graphite, Acta Mater 2013: 61; 3172–3185.
[107] Wang YZ, Li J. Phase field modeling of defects and deformation. Acta Mater 2010;58:1212–35.
[108] Chen LQ. Phase-field models for microstructure evolution. Annu Rev Mater Res 2002;32:113–40.
[109] Ma N, Dregia SA, Wang Y. Segregation transition and drag force at grain boundaries. Acta Mater 2003;51:3687–700.
[110] Boettinger WJ, Warren JA, Beckermann C, Karma A. Phase-field simulation of solidification. Annu Rev Mater Res 2002;32:163–94.
[111] Heo TW, Bhattacharyya S, Chen L-Q. A phase field study of strain energy effects on solute-grain boundary interactions. Acta Mater 2011; 59: 7800–7815.
[112] Trelewicz JR, Schuh CA. Grain boundary segregation and thermodynamically stable binary nanocrystalline alloys. Phys Rev B 2009;79:094112.
[113] Weissmüller J, Krauss W, Haubold T, Birringer R, Gleiter H. Atomic structure and thermal stability of nanostructured Y-Fe alloys. Nanostruct Mater 1992;1:439–47.
[114] Liu F, Kirchheim R. Nano-scale grain growth inhibited by reducing grain boundary energy through solute segregation. J Cryst Growth 2004;264:385–91.
[115] Liu F, Kirchheim R. Grain boundary saturation and grain growth. Scr Mater 2004;51:521–5.
[116] Darling KA, Chan RN, Wong PZ, Semones JE, Scattergood RO, Koch CC. Grain-size stabilization in nanocrystalline FeZr alloys. Scr Mater 2008;59:530–3.
[117] Detor AJ, Miller MK, Schuh CA. Solute distribution in nanocrystalline Ni–W alloys examined through atom probe tomography. Philos Magn 2006;86:4459–75.
[118] Farber B, Cadel E, Menand A, Schmitz G, Kirchheim R. Phosphorus segregation in nanocrystalline Ni–3.6 at.% P alloy investigated with the tomographic atom probe (TAP). Acta Mater 2000;48:789–96.
[119] Detor AJ, Miller MK, Schuh CA. Measuring grain-boundary segregation in nanocrystalline alloys: direct validation of statistical techniques using atom probe tomography. Philos Magn Lett 2007;87:581–7.
[120] Choi PP, Al-Kassab T, Gärtner F, Kreye H, Kirchheim R. Thermal stability of nanocrystalline nickel–18 at.% tungsten alloy investigated with the tomographic atom probe, Mater Sci Eng A 2003: 353; 74–79.
[121] Pradeep KG, Herzer G, Choi PP, Raabe D. Atom probe tomography study of ultrahigh nanocrystallization rates in FeSiNbBCu soft magnetic amorphous alloys on rapid annealing. Acta Mater 2014;68:295–309.
[122] Li YJ, Choi PP, Borchers C, Chen YZ, Goto S, Raabe D, et al. Atom probe tomography characterization of heavily cold drawn pearlitic steel wire. Ultramicroscopy 2011;111:628–32.
[123] Raabe D, Choi PP, Li YJ, Kostka A, Sauvage X, Lecouturier F, et al. Metallic composites processed via extreme deformation: Toward the limits of strength in bulk materials. MRS Bull 2010;35:982–91.
[124] Nakada N, Tsuchiyama T, Takaki S, Hashizume S. Variant selection of reversed austenite in lath martensite. ISIJ Int 2007;47:1527–32.
[125] Hickson MR, Hurley PJ, Gibbs RK, Kelly GL, Hodgson PD. The production of ultrafine ferrite in low-carbon steel by strain-induced transformation. Metall Mater Trans A 2002;33:1019–26.
[126] Krauss G. Martensite in steel: strength and structure. Mater Sc Eng A 1999;273–275:40–57.
[127] Ueji R, Tsuji N, Minamino Y, Koizumi Y. Ultragrain refinement of plain low carbon steel by cold-rolling and annealing of martensite. Acta Mater 2002;50:4177–89.
[128] Luo J. Developing interfacial phase diagrams for applications in activated sintering and beyond: current status and future directions. Am Ceram Soc 2012;95:2358.
[129] Wolf D. Atomic-level geometry of crystalline interfaces, Chapman & Hall, London. Mater Interfaces: Atomic-Level Struct Properties, 1992; 1–57.
[130] Lejcek P. Grain boundary segregation in metals. Berlin, Heidelberg: Springer Verlag; 2010.
[131] Gautam A, Ophus C, Lancon F, Radmilovic V, Dahmen U. Atomic structure characterization of an incommensurate grain boundary. Acta Mater 2013;61:5078–86.
[132] Elder KR, Katakowski M, Haataja M, Grant M. Modeling elasticity in crystal growth. Phys Rev Lett 2002;88:245701.
[133] Elder KR, Provatas N, Berry J, Stefanovic P, Grant M. Phase-field crystal modeling and classical density functional theory of freezing. Phys Rev B 2007;75:064107.